Lab on a Chip

Cite this: *Lab Chip*, 2012, **12**, 5007–5015

www.rsc.org/loc

PAPER

Monitoring the dynamics of primary T cell activation and differentiation using long term live cell imaging in microwell arrays†

Irina Zaretsky,‡ Michal Polonsky,‡ Eric Shifrut, Shlomit Reich-Zeliger, Yaron Antebi, Guy Aidelberg, Nir Waysbort and Nir Friedman*

Received 16th July 2012, Accepted 14th September 2012
DOI: 10.1039/c2lc40808b

Methods that allow monitoring of individual cells over time, using live cell imaging, are essential for studying dynamical cellular processes in heterogeneous cell populations such as primary T lymphocytes. However, applying single cell time-lapse microscopy to study activation and differentiation of these cells was limited due to a number of reasons. First, primary naïve T cells are non-adherent and become highly motile upon activation through their antigen receptor. Second, $CD4^+$ T cell differentiation is a relatively slow process which takes 3–4 days. As a result, long-term dynamic monitoring of individual cells during the course of activation and differentiation is challenging as cells rapidly escape out of the microscope field of view. Here we present and characterize a platform which enables capture and growth of primary T lymphocytes with minimal perturbation, allowing for long-term monitoring of cell activation and differentiation. We use standard cell culture plates combined with PDMS based arrays containing thousands of deep microwells in which primary $CD4^+$ T cells are trapped and activated by antigen coated microbeads. We demonstrate that this system allows for live cell imaging of individual T cells for up to 72 h, providing quantitative data on cell proliferation and death times. In addition, we continuously monitor dynamics of gene expression in those cells, of either intracellular proteins using cells from transgenic mice expressing fluorescent reporter proteins, or cell surface proteins using fluorescently labeled antibodies. Finally, we show how intercellular interactions between different cell types can be investigated using our device. This system provides a new platform in which dynamical processes and intercellular interactions within heterogeneous populations of primary T cells can be studied at the single cell level.

Introduction

The ability to follow dynamic cellular processes using live cell imaging has led to advances in our understanding of cell signaling and gene expression dynamics within heterogeneous cell populations.[1–5] However, this methodology is hard to implement for specific cell types, limiting investigation of dynamic processes at the single cell level. In particular, live cell imaging of primary T cells in culture is challenging, due to their non-adherent nature, and their high motility upon activation through their antigen receptor. Conventional techniques for single cell research, such as flow cytometry, allow for measurements of multiple parameters with single cell resolution at a given time point. However, this analysis cannot provide long-term dynamical data on individual T cells.

Department of Immunology, Weizmann Institute of Science, Rehovot 76100, Israel. E-mail: ira.zaretsky@weizmann.ac.il; michal.polonsky@weizmann.ac.il; nir.friedman@weizmann.ac.il; Fax: +927-8-9343657; Tel: +927-8-9346294

† Electronic supplementary information (ESI) available. See DOI: 10.1039/c2lc40808b

‡ These authors contributed equally to this work.

Microfluidics devices have been beneficial for single cell studies, including the use of microwell arrays for capture and imaging of non-adherent cells.[6–15] These devices were recently used for culturing and monitoring of T cell lines as well as primary T cells.[14–19] However, these studies followed cells dynamically for a limited time (from tens of minutes up to ~24 h)[7,9] or used microwells as a tool for separating cells in order to perform other assays such as cytokine secretion[10,16] or evaluation of cytotoxicity of $CD8^+$ T cells.[15,20] We set out to construct a microwell platform that will enable studying the dynamics of activation and differentiation of primary $CD4^+$ T cells with single cell resolution and over extended periods of time, as required by the long time scale of these processes.

Naïve $CD4^+$ T cells can differentiate into a number of lineages, each having a specific immune function.[18,21,22] The differentiation process involves expression of lineage specific genes, cell proliferation leading to clonal expansion and also cell death. Single cell studies could provide insightful data on this process as there is a high level of heterogeneity between differentiating cells, even when subjected to identical differentiation driving conditions. There are some major difficulties in

realizing live cell imaging of primary T cells during activation and differentiation. First, these cells are non-adherent; second, upon activation cells grow in size and become highly motile; third, these cells tend to form clusters after activation both *in vivo*[23] and *in vitro*;[24] Finally, the differentiation process takes several days, so in order to fully characterize it cells need to be monitored for long periods of time. Following these processes *in vivo*, *e.g.* using two-photon imaging, is challenging as cells move out of the observation region, and also since current techniques do not allow monitoring for few days. $CD4^+$ T cell activation and differentiation can be induced and studied *in vitro*, complementing *in vivo* studies and yielding mechanistic information on the related molecular and cellular processes. Hence, we aimed to construct an *in vitro* culture system that will overcome the abovementioned difficulties and will allow for monitoring of $CD4^+$ T cells during the course of activation and differentiation (3–4 days) using time-lapse movies. We required that the system would enable the evaluation of phenotypic changes which occur during the process. These include extraction of times of cell proliferation and cell death, as well as temporal patterns of expression of specific proteins in individual cells.

We combined soft-lithography based microwell arrays (MWA) with standard cell culture plates, facilitating their use in time lapse microscopy setups without need for specialized holders and using standard cell culture equipment and conditions. Our device is based on a thin layer of PDMS that contains an array of microwells, which can vary in size and depth, and is placed at the bottom of an optical 96-well plate. We show that T cells remain viable in the MWA and can proliferate and differentiate upon activation with antigen coated microbeads. Thus, these MWAs are suitable for high-throughput microscopic studies of thousands of T cells, monitoring the dynamics of their proliferation, death, and expression of activation and differentiation markers, and evaluating cell-to-cell variability of these parameters. In addition, these devices allow for investigation of intercellular interactions, as the relative positions of cells in the culture are known and remain stable during an experiment.

Experimental

Microwell array design and fabrication

Photolithography masks were designed using autoCAD (Autodesk, San Rafael, CA). Different molds were designed, containing microwells with diameters of 25, 40, 60 and 300 μm. Each MWA contains between a few tens to tens-of-thousands of hexagonally spaced microwells (depending on microwell size). The depth of the microwells was established experimentally for primary T cells at 40 μm in the smaller microwells and 60 μm for the 300 μm microwells. This depth of microwells is 3–4 times the cell diameter, thus reducing escape of activated cells, which is notable in shallower microwells.

Molds were fabricated using a negative photoresist (SU8-3025, Microchem Corporation, Newton, MA) on mech grade 3′′ silicon wafers (University wafer Inc, Boston MA). First, wafers were cleaned using RCA protocol[25] and photoresist was poured and spun to yield feature heights of 40 μm or 60 μm. Next, wafers were exposed to UV irradiation on a contact mask aligner using a dark-field mask printed at 50 000 dpi (FineLine, Colorado Springs, CO). Photoresist was then hardened using standard techniques,[26] and wafers were treated with hexamethyldisilazane (Sigma Aldrich, St. Louis, MO).

PDMS (Sylgard 184, Dow Corning, Midland, MI) was mixed in 10 : 1 weight ratio (base : curing agent), 3 ml were poured on the template wafer and spun for 30 s at 1500 rpm (1000 rpm) for the 25–60 μm (300 μm) microwells. Spinning assures a thin PDMS bottom of the microwells, which is required to allow for the operation of the automated focus system of our microscope (Nikon TiE). Wafer was baked for 30 min at 80 °C until PDMS is fully cured. After curing, the thin PDMS layer was cut to stripes, peeled and gently placed on stripes of a thick PDMS slice such that the top of the microwells is facing the thick PDMS. This thick PDMS serves as a helping tool to place the thin layer containing the MWA into a 96-well. Small squares ($\sim$5 mm $\times$ 5 mm) containing the microwell pattern were cut and punched into an optical bottom 96-well plate (Thermo Fisher Scientific, Rochester, NY) using tweezers. As the thin layer adheres strongly to the bottom of the plate, it detaches from the thick layer and remains inside the 96-well. This process is schematically described in Fig. 1a–d.

Cells

C57BL/6 mice were obtained from Harlan Laboratories (Rehovot, Israel) and Foxp3-GFP mice were kindly provided by Vijay Kuchroo (Harvard Medical School). All mice were maintained at the Weizmann Institute animal facilities and were cared for in accordance with national and institutional guidelines. Experiments were approved by the Institutional Animal Care and Use Committee. Splenocytes were collected from 5 to 12 week old mice. Erythrocytes were osmotically lysed and single-cell suspensions were incubated with $CD4^+$ T cell biotin antibody cocktail followed by incubation with anti-biotin microbeads (Miltenyi Biotec, Germany). $CD4^+$ T cells were then purified by magnetic isolation with an AutoMACS sorter (Miltenyi Biotec, Germany). For isolation of $CD4^+$ $CD62L^+$ naïve T cells, the purified $CD4^+$ T cell suspension was incubated with anti-CD62L microbeads followed by separation with the AutoMACS. In all experiments >95% of these cells were positive for $CD4^+$ and CD62L, as verified by flow cytometry. Cells were cultured in complete RPMI 1640 medium w/o phenol red, supplemented with 10% (vol/vol) FCS, 100 U/ml of penicillin, 100 mg ml^{-1} of streptomycin, 2 mM glutamine, 10 mM HEPES, 1 mM sodium pyruvate and 50 mM β-mercaptoethanol, all from biological industries (Beit Haemek, Israel). During the experiments, cells were activated with anti-CD3 and anti-CD28 coated microbeads (Invitrogen – Molecular probes, Grand Island, NY), and growth medium was supplemented with 5 ng ml^{-1} recombinant mouse IL-2 (R&D systems, Minneapolis, MN). To drive differentiation of naïve $CD4^+$ T cells to a regulatory phenotype (Treg cells), growth medium was supplemented also with 10 ng ml^{-1} of recombinant human TGFβ (R&D systems, Minneapolis, MN). In some experiments cells were stained with PE labeled anti-CD69L (MEL-14, eBioscience, San Diego, CA).

Cell loading into the MWA

To facilitate cell loading into the small volume microwells and eliminate trapped air bubbles that remain in the microwells due to the hydrophobicity of PDMS, wells were filled with 200 μl

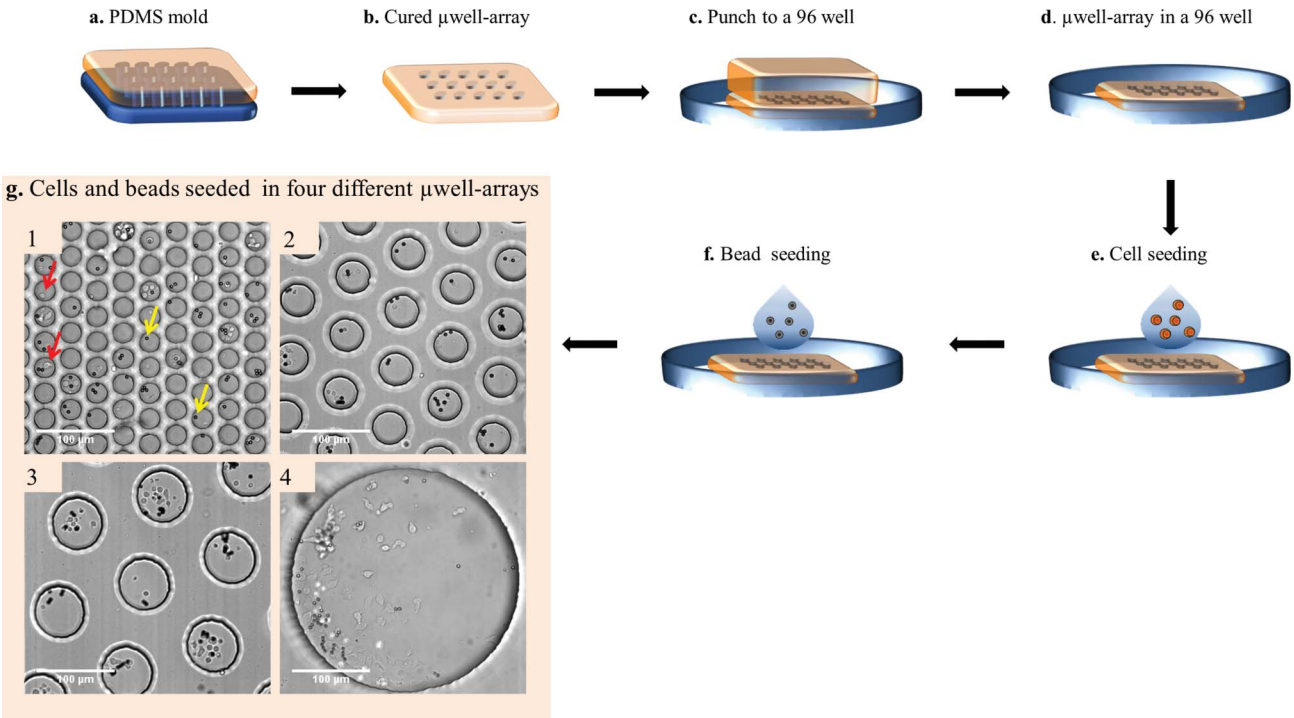

Fig. 1 MWA fabrication and cell loading. (a–f) Schematics of the fabrication and seeding process: a) PDMS polymer is poured onto a photolithographically patterned master and spun to achieve desired thickness. b) After curing, the thin PDMS layer (~90 μm thick) is peeled off and the MWA is cut out. c) The thin PDMS layer containing the MWA is placed on a thick PDMS-made holder and punched into an optical bottom 96-well plate. d) The PDMS holder is removed leaving the microwell-array attached to the bottom of the 96-well. e) Cell suspension is placed in the 96-well and the plate is spun to allow efficient settling of T cells into the microwells. Excess cells are removed. f) Activation microbeads (anti-CD3/anti-CD28) are introduced into the 96-well and left to settle into the microwells. Excess beads are removed and fresh medium is introduced. g) Representative images of primary mouse $CD4^+$ T cells and activation beads in 4 different designs of the MWA (representative cells are marked with red arrows and beads with yellow arrows): 1. microwell diameter = 25 μm, microwell depth = 40 μm. 2. Diameter = 40 μm, depth = 40 μm. 3. Diameter = 60 μm, depth = 40 μm 4. Diameter = 300 μm, depth = 60 μm.

PBS and left at 4 °C overnight. The plate was then placed in vacuum for 1 h and centrifuged for 1 min (1300 rpm) to remove residual bubbles. Then, cells were loaded into the MWA, followed by loading of the activation microbeads. First, PBS was removed and a tissue culture medium with the desired amount of primary naïve $CD4^+$ T was added to each 96-well containing the MWA. Cells were allowed to settle by spinning the plate at 1300 rpm for 1 min (Fig. 1e). Residual cells were aspirated and medium containing anti-CD3/anti-CD28 coated activation microbeads was loaded into the wells (Fig. 1f). Anti-CD3/anti-CD28 supply both TCR activation and co-stimulatory signals, thus allowing *in vitro* T cell activation independent of antigen specificity.[27] Following this activation cells grow in size and proliferate. We found that upon activation, T cells remain in proximity of the microbeads, thus stay within the microwells allowing for their long term imaging. The combination of deep microwells and activation microbeads also prevents extensive cell clustering, which is observed in standard *in vitro* culture of T cells (see Fig. S3, ESI†). We also tried to activate T cells by coating the MWA with anti-CD3/anti-CD28 antibodies. However, under this mode of activation T cells could escape the microwells, even when their depth (40–60 μm) was few times larger than the typical diameter of an activated T cell (~15 μm). Fig. 1g shows images of primary mouse $CD4^+$ T cells and activation beads inside MWAs of different diameters and depths.

Microscopy

For time-lapse experiments we used a Ti-eclipse microscope (Nikon Instruments) equipped with an automated stage, an incubator, and a closed chamber that allows for CO_2 flow over the 96-well plate. Cells were imaged using 20× objective and monitored using bright field illumination and three fluorescence channels: FITC, Cy3 and TxRed. Time-lapse movies were collected using the NIS-elements software (Nikon Instruments).

Analysis of cell division times and gene expression

In order to obtain quantitative single cell data, images were analyzed using a semi-automated MATLAB (MathWorks, Natick, MA) based custom code. The code identifies the location of each microwell in the array and visualizes each one separately. The individual microwells are then analyzed manually for cell numbers and division times. If the cells are fluorescently stained or express a fluorescent protein, the software also calculates the background corrected mean fluorescence intensity (MFI) in each microwell at each time-point.

Analysis of cell death times

For evaluation of cell death events, we added a low concentration (0.25 μg ml^{-1}) of the DNA intercalating dye Propidium Iodide (Sigma-Aldrich St. Louis, MO) to the cell culture medium

at the starting time of the experiment. Propidium iodide (PI) is not fluorescent in solution and does not penetrate the plasma membrane of viable cells. Upon cell death, PI quickly stains the DNA of the cell giving rise to a strong fluorescence signal. We automatically evaluated the time of elevation in the cell's fluorescence in the red (TxRed) channel using a custom MATLAB code. Briefly, images for each microwell were processed using watershed type algorithm, to detect dead cells. At each time point, the number of dead cells per microwell was counted and the times of death were determined. The algorithm was manually validated on sampled microwells.

Results and discussion

Distribution of cells and beads in the MWA

Our loading scheme results in a random distribution of cells and activation beads in the MWA. Since we are mainly interested in following single cells, it is important to calibrate the average numbers of cells and beads in the loading medium that result in appropriate numbers of cells and beads in the microwells. Additionally, we wanted to verify that the loading scheme is not affected by cell adhesion and clustering, which may reduce the number of microwells containing a single cell. Here, we describe the distributions of cells and activation beads in MWAs which contain microwells that are 25–60 μm in diameter and are 40 μm deep. We found that seeding of 25 000 cells per 96 well plate for the 25 μm MWA, and 12 500 cells per 96 well plate for the 40 and 60 MWAs, gave optimal loading of microwells containing a single cell. Under these conditions, the average occupancy was 0.66 cells per microwell for the 25 μm MWA and 1.65 cells per microwell for the 40 μm MWA. The distributions of the number of cells per microwell and the number of beads per microwell both follow Poisson distributions (Fig. 2a–d), indicating that cells and beads are spread randomly into the microwells and clustering of beads or cells during the loading process is not significant. Under these conditions 30% (26%) of the microwells contain one cell, 55% (26%) are empty, and 15% (48%) contain two or more cells, for the 25 μm (40 μm) MWA.

Other than being able to monitor single cell behavior, our seeding protocol also allow us to achieve multiple culture conditions such as one cell and one bead, two cells and one bead, *etc.*, within the same 96 well plate. This enables culture of cells which are all exposed to the same cytokines (*i.e.* IL-2, TGFβ *etc.*) but differ in their microenvironment. This inherent variability also allows for internal controls, such as cells without activation beads in their microwell, being cultured under the same conditions as the activated cells. We demonstrate this in Fig. 2f,g, which shows the co-distributions of cells and beads in MWAs of 25 μm diameter (f) and 40 μm diameter (g). We also found that the mean microwell occupancy linearly increased with the number of seeded cells, for all microwell diameters tested (Fig. 2e). This linear dependency together with the observed Poisson distributions allows for calculation of the required initial seeding numbers that will give a desired distribution of cells/beads per microwell.

Long term culture of primary T cells in MWAs

The above design allowed for culturing and quantitative analysis of primary mouse T cells for up to 72 h in the MWA. We first assessed cell survival and proliferation, by counting the number of live cells per microwell at the end of the culturing period. Fig. 3a shows cell numbers in the two MWAs (25 μm and 40 μm) after 72 h of culture. Only microwells that initially contained one cell and at least one bead are included in this analysis. The high fraction of empty microwells at this time point is indicative of substantial cell death, which occurs also in conventional tissue culture of these cells, mainly during the first 48 h (Fig. S1, ESI†). On the other hand, we find that ~10% of the microwells that originally had one cell, contained two or more cells at the end of the culture, indicating cell proliferation. The distribution of final cell numbers is broad, with some microwells containing up to 6 cells in the 25 μm MWA and up to 10 cells in the 40 μm MWA. Interestingly, this distribution is non-monotonic; in both experiments the fraction of microwells containing 3 cells is lower than those containing 4 cells. As we show below, this is caused by the high level of synchronization in division times of daughter cells. It is possible that some of the 25 μm microwells contained more cells than we counted but we could not tell these cells apart, as they form large clumps in the final hours of the experiment. This is less severe in the larger 40 μm microwells, which can accommodate a larger number of cells at their bottom. Fig. 3b shows representative images of microwells containing different numbers of cells at the end of the experiment, all of which started with one cell and at least one activation bead. Dead cells are strongly fluorescent (red) due to the added propidium iodide (PI) at the beginning of the experiment (see above for a detailed staining protocol).

Continuous monitoring of individual cells allows for precise determination of times of cell division and cell death (see movies S1-3 for representative microwells, ESI†). We measured cell division and death times by following individual clones starting from one cell. Division times were obtained in a semi-automatic manner using our image analysis tool. PI staining of dead cells allowed for automated identification of exact death times from time lapse movies as described above. Fig. 3c shows images of a typical microwell over the course of an experiment. The microwell initially contains one T cell and one bead; 31 : 20 h after the beginning of the experiment the cell has divided; then (around 42 h) one daughter cell has died as judged by the increase in PI staining, while the other one divided immediately after; the two daughter cells divided again around 61 h. Fig. 3d shows a graphical representation of death and division events that occurred in this microwell.

For each microwell in the array, a timelined lineage tree is evaluated from the times of proliferation and death events, in a similar manner. This data is used for high-throughput analysis of the differences and correlations between cell progenies during the course of their development, as shown in the next section.

MWA enables precise analysis of T cell division and death times

Proliferation of T cells following their activation forms the basis for clonal expansion.[28] The MWAs provide an experimental system in which these processes can be quantified with high throughput following many cell lineages in parallel. The measurement of cell death times at high temporal resolution allowed us to determine cell death rate during the course of the experiment. This rate is given by the fraction of live cells at time

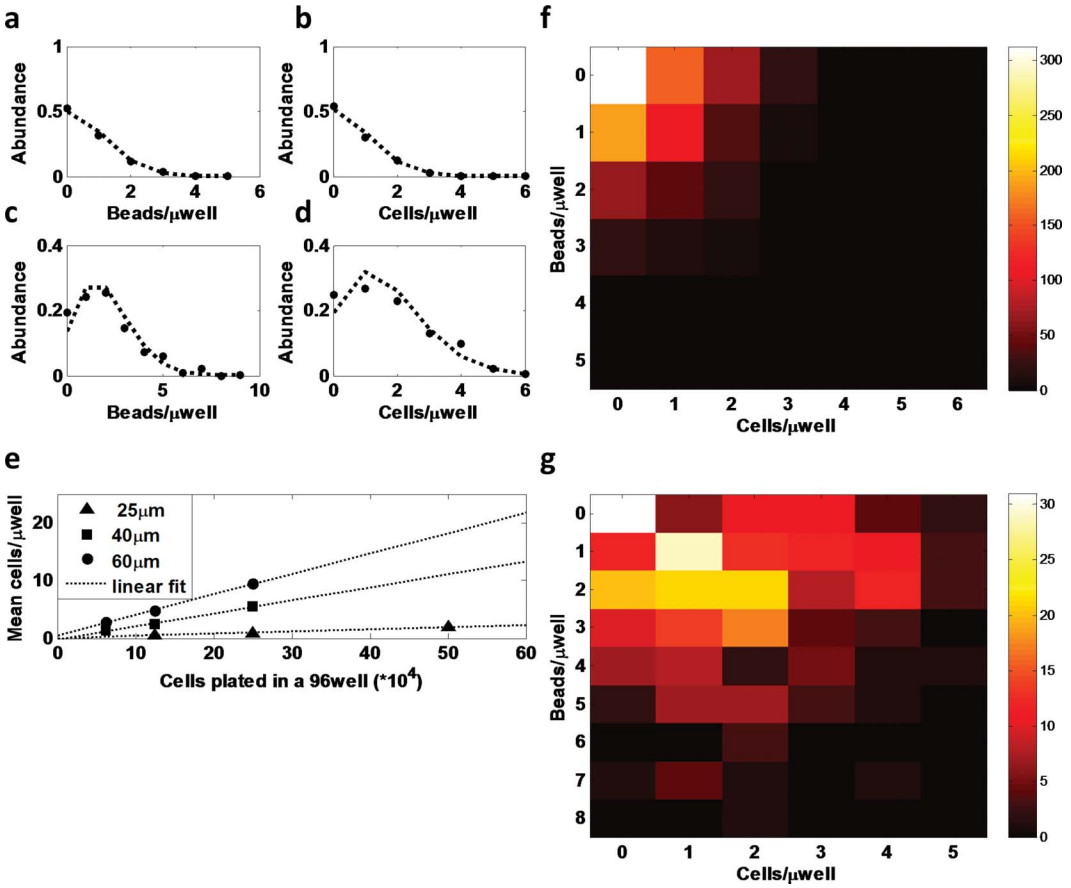

Fig. 2 Measured distributions of cells and beads in MWAs. a–b) 25,000 T cells and 20 000 beads were seeded in a 96-well containing a 25 μm MWA. a) Distribution of the measured numbers of beads/microwell. b) Distribution of the measured numbers of cells/microwell. Experimental data (dots) is well fitted by a Poisson distribution (dotted line). c–d) 12 500 cells and 20 000 beads were seeded in a 96-well containing a 40 μm MWA. c) Same as in a. d) same as in b. e) Mean number of cells/microwell plotted against the initial number of cells seeded per 96 well, for MWAs with different microwell diameters (25, 40 and 60 μm). Mean microwell occupancy increases linearly with seeded cell number with $R^2 = 0.99$ for the three diameters. The mean number of cells/microwell increases in proportion to microwell area. f) Co-distribution of beads/microwell and cells/microwell in the 25 μm MWA. Colorbar represents the number of microwells containing the specific cells/beads combination from the same experiment as in a–b. g) Co-distribution of beads/microwell and cells/microwell in the 40 μm MWA. Data from the same experiment as in c–d.

T that were identified as dead at time $T + \Delta T$. We plot in Fig. 4a the cell death rate as a function of time in culture, for cells that were in microwells devoid of microbeads or in microwells containing microbeads. During the first 15 h a similar death rate is observed for both classes of cells, starting at $\sim 0.06\ h^{-1}$, and declining to $\sim 0.025\ h^{-1}$. Hence, during these early times of culture cell death is independent of TCR activation. This initial cell death might be caused by an initial shock that the cells experience after being extracted from the spleen and transferred to an *ex-vivo* culture. After ~ 15 h the death rate of the activated cells keeps decreasing and stabilizes at 0.005–0.01 h^{-1}, while the death rate of non-activated cells gradually increases. As mentioned earlier, both cell classes (activated and non-activated) grow in the same 96 well plate, thus share the same medium. Such quantitative determination of cell death rate, its change over time in culture and its dependence on TCR activation can only be obtained from tracking of individual cells over time, as demonstrated here using our MWAs and live cell imaging approach.

We continue by evaluation of cell division times during activation, and their statistical properties. Fig. 4c–e shows analysis of division times for T cells cultured in MWAs. Only microwells that initially contained one cell and at least one activation microbead were included in the analysis. Fig. 4e shows the distribution of division times for the 1st division, corresponding to the initial cell, and for the 2nd and 3rd divisions, which correspond to division of its two daughter cells. The mean time for first division is 43.3 h, which is consistent with existing data (~ 45 h).[29,30] The distribution of the time for the 1st division is relatively broad, with SD = 15.1 h. The 2nd and 3rd divisions follow highly similar distributions, with mean of 50.1 h (51.3 h) and SD of 14.6 h (15.0 h), respectively. This indicates a high level of synchronization in the division of the two daughter cells. Indeed, the correlation between division times of the two daughter cells is very high, and in most cases the two daughter cells divide within 15–20 min of each other (Fig. 4c). A similar synchronization between daughter cells was recently observed also for B cells.[12,31] The mean duration of the cell cycle of the second cell generation is 14.1 h with SD = 4.6 (Fig. 4f). This is in agreement with existing data (~ 12–18 h), where generation time was inferred from flow cytometry measurements.[29,30,32] Finally, we found weak correlation ($R^2 = 0.45$, $P = 0.01$) between the 1st

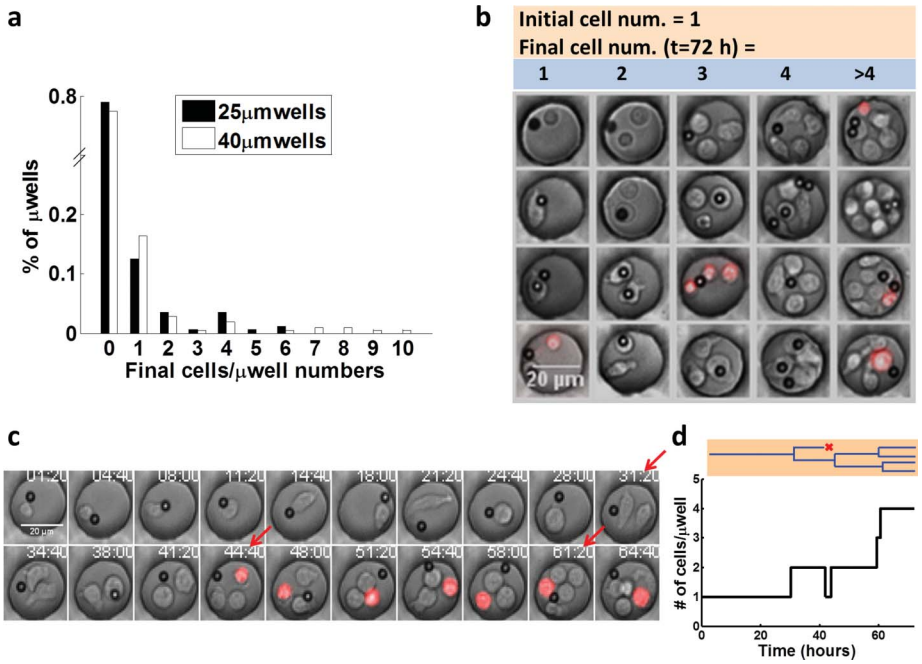

Fig. 3 Cell proliferation and survival in MWAs. a) Distribution of the final number of live cells after 72 h of culture, in 25 μm microwells (black bars) and 40 μm microwells (white bar). All microwells in this analysis initially contained one cell and at least one activation bead. Empty microwells (final cell number = 0) indicate a cell that died during the experiment. microwells with a final cell number >1 indicate proliferation. b) Representative microscope images (bright field and PI channel overlay) of 20 microwells after 72 h culture. All microwells (25 μm in diameter) initially contained one T cell and at least one activation bead, but harbor different cell numbers at the end of the experiment due to cell division and death events. Dead cells are identified by PI staining and appear in strong red. c) Microscope images of a typical microwell sampled over the course of a 72 h experiment. Division events are marked with red arrows. A dead cell is identified by PI staining and appears in strong red from 44 : 40 h. d) Time trace depicting the number of live cells in the microwell shown in c (bottom) and the corresponding timelined lineage tree of the cell progeny (top).

and 2nd division times (Fig. 4d), that is, between daughter cells and their mothers. This correlation suggests that the time for division of daughter cells is affected by internal properties of the mother naïve T cell, unlike the behavior found for B cells, in which mother–daughter correlation in division times was observed only for subsequent cell generations.[31]

Measuring dynamics of gene expression in individual primary T cells activated in MWAs

Live imaging of primary T cells in MWAs allowed us to realize long-term dynamic measurements of gene expression in single T cells, following cells behavior continuously. Such analysis is not possible using common high-throughput singe cell techniques such as flow cytometry, which sample cell populations at discrete time points. We focused on dynamical changes in gene expression that occur during T cell activation and differentiation. We followed gene expression either using continuous staining of cell surface molecules inside the MWA, or using fluorescent proteins as reporters for gene expression.

Fig. 5a shows images from a time-lapse movie of a 25 μm microwell containing a naïve $CD4^+$ T cell that received stimulation with two microbeads. We measured the level of the cell surface molecule CD69, which is up-regulated following T cell activation.[33] To allow for continuous monitoring, 0.1 μg ml^{-1} of PE conjugated anti-CD69 antibody was added to the cell culture medium. At this concentration, elevation in background fluorescence is small. Once cells elevate CD69 levels, the added antibodies accumulate on the cell surface providing a fluorescent signal that can be distinguished from the background. This fluorescent signal dynamically changes with levels of its target molecule (CD69 in this case) on the cell surface.[12] Traces of CD69 dynamic elevation were quantified in individual microwells using our in-house MATLAB based code (Fig. 5b, see also methods section). CD69 levels rise upon activation in a fast rate for the first 10–20 h, and tend to level off towards 40 h (end of experiment). Individual cells, however, show different dynamics of CD69 elevation.

Fig. 5c demonstrates dynamic monitoring of gene expression using a fluorescent reporter gene. Here, primary naïve T cells were extracted from a transgenic mouse which expresses GFP fused to the transcription factor Foxp3, which plays a key role in differentiation of regulatory T cells (Tregs).[34,35] Cells were seeded in the MWA and were induced into Treg differentiation by adding the cytokines TGFβ and IL-2 to the growth medium. First, we verified that Foxp3-GFP expression during Treg differentiation in the MWA evolves in a very similar manner to that measured in conventional tissue culture (Fig. S2). Expression of Foxp3 in the microwell presented in Fig. 5c starts around 30 h after activation, close to the time of first cell division. The total GFP fluorescence in few microwells is plotted in Fig. 5d, showing a steady increase from 30 h to 72 h (end of experiment).

The MWAs can also be used to study cell–cell interactions, for example by loading and co-culturing cells of different types. The ordered structure of the array provides a controlled microenvironment in which cells can interact with the same neighbors

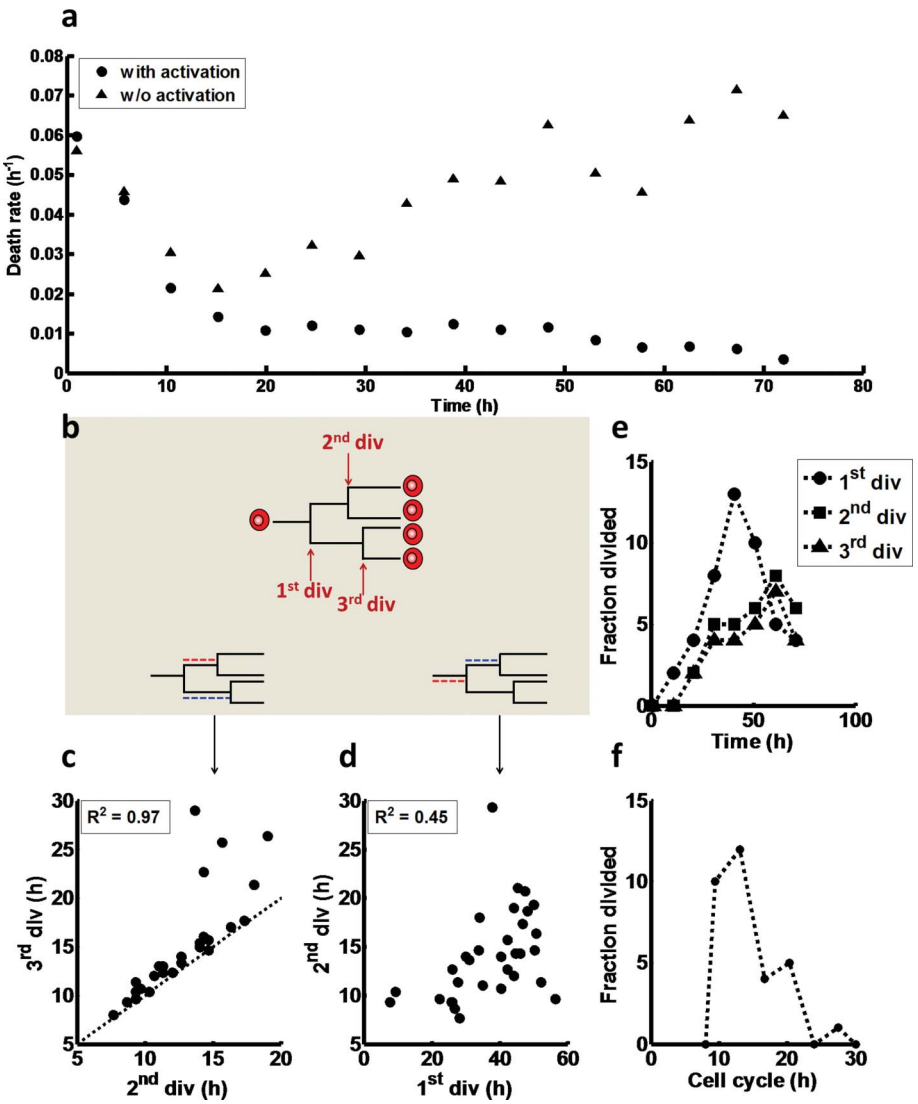

Fig. 4 Quantitative evaluation of death and proliferation events. a) Rate of cell death during the experiment for cells that were activated (dots, at least one activation bead in microwell) and for un-activated cells (triangles, no activation beads in microwell). b) Schematic description of proliferation analysis. Red and blue lines indicate the different time intervals plotted in c–d. Red line describes time intervals plotted on the x axis, blue line is plotted on the y axis. c) Division times of daughter cells are synchronized: Time of the 3rd division plotted against the time of the 2nd division. Only microwells initially containing one cell and at least one activation microbead were included in the analysis (for 25 μm and 40 μm diameter microwells, combined). Most division events fall around the trend line ($x = y$). Correlation coefficients is $R^2 = 0.97$ (excluding the 5 outliers). d) Time of the 2nd division (daughter cell) plotted against the time of the 1st division (mother cell). Correlation coefficients is $R^2 = 0.45$. e) Distribution of division times for all cells (mean and SD values are described in the text). f) Distribution of the generation time of daughter cells.

during an experiment. In Fig. 5e we demonstrate a suppression assay between regulatory and effector T cells performed within a MWA. The aim of this assay is to investigate suppressive ability of Tregs on effector T cells by reducing their proliferation and/or increasing their death rate. Specifically, Fig. 5e shows an example of a microwell that initially contained one Treg and one effector T cell activated by one microbead. The Treg expresses Foxp3-GFP, and proliferates. The effector cell does not divide, and eventually dies ($\sim$32 h). As our seeding protocol allows different combinations of the two cell types, it is possible to monitor in parallel interactions between the two cell types with different combinations of cells in each microwell, all grown in the same 96 well. This can be combined with monitoring of gene expression dynamics, as described above, to characterize for example activation or differentiation of the effector T cells, together with the suppressive effect of the regulatory cells.

Conclusions

We demonstrated a new method for imaging and single cell analysis of primary T cells over long time periods. We combined microfluidics technology with standard cell culture methods to fabricate a large array of deep microwells placed on the bottom of a standard 96 well plate, in which thousands of T cells can be investigated in parallel. T cells are activated within the microwells using antibody coated microbeads which also maintain motile activated T cells within the microwells for several days. Using custom made image analysis tools we were

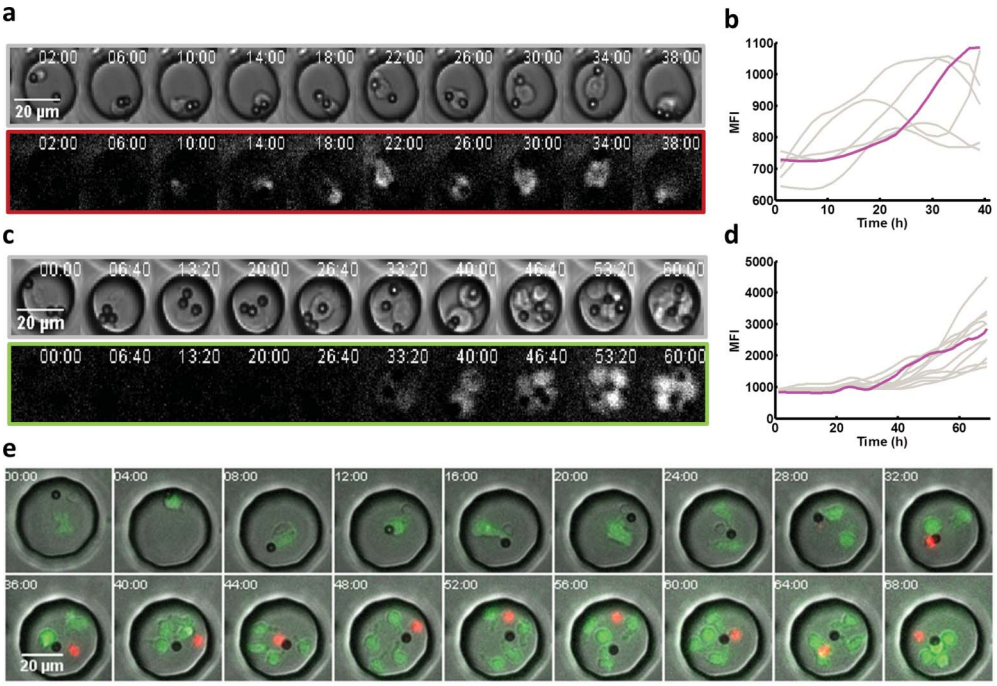

Fig. 5 Dynamics of gene expression in individual T cells cultured in a MWA. a) Measurement of CD69 up-regulation following T cell activation by continuous staining. Naïve mouse $CD4^+$ T cells were seeded into a MWA and cultured in the presence of activation microbeads. PE-conjugated anti-CD69 antibody was added to the growth medium at 0.1 μg ml^{-1}, allowing for continuous monitoring of CD69 levels on the surface of the cell. Images of one microwell which initially contained one T cell and two beads are shown (Top: bright field; Bottom: PE fluorescence). b) MFI of the microwell depicted in 5a during the course of the experiment (magenta) and of 4 other microwells from the same experiment (gray). c) Measurements of Foxp3 up-regulation during differentiation of induced regulatory T cells. Naïve T cells from a transgenic mouse expressing Foxp3-GFP fusion were seeded into a MWA and cultured in the presence of activation microbeads. TGFβ and IL-2 were added to the growth medium to drive Treg differentiation. Images of one microwell that initially contained one T cell and three beads are shown (Top: bright field; Bottom: GFP fluorescence). d) MFI of the microwell depicted in 5c during the course of the experiment (magenta) and of 10 additional microwells from the same experiment (gray). e) Images of a suppression assay between a regulatory T cell (Foxp3-GFP, green) and a naïve effector T cell (un-stained) in a 40 μm MWA over the course of a 72 h experiment. The regulatory T cell proliferates and preserves its Foxp3 expression, while the effector cell dies (at ~32 h) as indicated by PI staining (red).

able to quantify proliferation and death events and track dynamic changes in reporter gene expression. Thus, these microwell arrays offer new possibilities for single cell dynamic analysis of T cell activation and differentiation, and investigation of the roles of intercellular interactions in shaping these processes.

Acknowledgements

We thank Alexander Yoffe and Sharon Garusi from the Department of Chemical Research Support for help with template fabrication. We thank Jacob Rimer and Inbal Eizenberg for comments on the manuscript. This research was supported by the European Union 7th Framework Programme as part of the project NanoII (grant agreement no. 229289); by The Converging Technologies Program of the Israel Science Foundation (grant no. 1752/07); and by the Israel Science Foundation (grant no. 1254/11). NF is incumbent of the Pauline Recanati Career Development Chair of Immunology.

References

1 H. H. McAdams and A. Arkin, Stochastic mechanisms in gene expression, *Proc. Natl. Acad. Sci. U. S. A.*, 1997, **94**, 814–9.
2 G. Lahav, *et al.* Dynamics of the p53-Mdm2 feedback loop in individual cells, *Nat. Genet.*, 2004, **36**, 147–50.
3 L. Cai, N. Friedman and X. S. Xie, Stochastic protein expression in individual cells at the single molecule level, *Nature*, 2006, **440**, 358–62.
4 J. T. Mettetal, D. Muzzey, J. M. Pedraza, E. M. Ozbudak and A. van Oudenaarden, Predicting stochastic gene expression dynamics in single cells, *Proc. Natl. Acad. Sci. U. S. A.*, 2006, **103**, 7304–9.
5 B. Munsky, G. Neuert and A. van Oudenaarden, Using gene expression noise to understand gene regulation, *Science*, 2012, **336**, 183–7.
6 J. R. Rettig and A. Folch, Large-scale single-cell trapping and imaging using microwell arrays, *Anal. Chem.*, 2005, **77**, 5628–34.
7 J. Doh, M. Kim and M. F. Krummel, Cell-laden microwells for the study of multicellularity in lymphocyte fate decisions, *Biomaterials*, 2010, **31**, 3422–8.
8 N. Zurgil, *et al.*, Polymer live-cell array for real-time kinetic imaging of immune cells, *Biomaterials*, 2010, **31**, 5022–9.
9 K. Guldevall, *et al.*, Imaging immune surveillance of individual natural killer cells confined in microwell arrays, *PLoS One*, 2010, **5**, e15453.
10 J. C. Love, J. L. Ronan, G. M. Grotenbreg, A. G. van der Veen and H. L. Ploegh, A microengraving method for rapid selection of single cells producing antigen-specific antibodies, *Nat. Biotechnol.*, 2006, **24**, 703–7.
11 M. Rottmar, M. Håkanson, M. Smith and r. K. Maniura-Webe, Stem cell plasticity, osteogenic differentiation and the third dimension. Journal of materials science, *J. Mater. Sci.: Mater. Med.*, 2010, **21**, 999–1004.
12 K. R. Duffy, *et al.*, Activation-induced B cell fates are selected by intracellular stochastic competition, *Science*, 2012, **335**, 338–41.
13 D. Day, *et al.*, A method for prolonged imaging of motile lymphocytes, *Immunol. Cell Biol.*, 2009, **87**, 154–8.

14 S. Faley, *et al.*, Microfluidic platform for real-time signaling analysis of multiple single T cells in parallel, *Lab Chip*, 2008, **8**, 1700–12.
15 Y. S. Schiffenbauer, *et al.*, A cell chip for sequential imaging of individual non-adherent live cells reveals transients and oscillations, *Lab Chip*, 2009, **9**, 2965–72.
16 Q. Han, *et al.*, Polyfunctional responses by human T cells result from sequential release of cytokines, *Proc. Natl. Acad. Sci. U. S. A.*, 2012, **109**, 1607–12.
17 S. Kobel, A. Valero, J. Latt, P. Renaud and M. Lutolf, Optimization of microfluidic single cell trapping for long-term on-chip culture, *Lab Chip*, 2010, **10**, 857–63.
18 C. A. London, A. K. Abbas and A. Kelso, Helper T cell subsets: heterogeneity, functions and development, *Vet. Immunolo. Immunopathol.*, 1998, **63**, 37–44.
19 J. Zhu and W. E. Paul, Peripheral $CD4^+$ T-cell differentiation regulated by networks of cytokines and transcription factors, *Immunol. Rev.*, 2010, **238**, 247–62.
20 N. Varadarajan, *et al.*, A high-throughput single-cell analysis of human $CD8^+$ T cell functions reveals discordance for cytokine secretion and cytolysis, *J. Clin. Invest.*, 2011, **121**, 4322–31.
21 J. J. O'Shea and W. E. Paul, Mechanisms underlying lineage commitment and plasticity of helper $CD4^+$ T cells, *Science*, 2010, **327**, 1098–102.
22 J. Zhu and W. E. Paul, Peripheral $CD4^+$ T-cell differentiation regulated by networks of cytokines and transcription factors, *Immunol. Rev.*, 2010, **238**, 247–62.
23 M. J. Miller, O. Safrina, I. Parker and M. D. Cahalan, Imaging the single cell dynamics of $CD4^+$ T cell activation by dendritic cells in lymph nodes, *J. Exp. Med.*, 2004, **200**, 847–56.
24 C. A. Sabatos, *et al.*, A synaptic basis for paracrine interleukin-2 signaling during homotypic T cell interaction, *Immunity*, 2008, **29**, 238–48.
25 W. Kern and D. A. Poutinen, Cleaning solutions based on hydrogen peroxide for use in silicon semiconductor technology, *RCA rev.*, 1970, 187–206.
26 A. Rosenthal, A. Macdonald and J. Voldman, Cell patterning chip for controlling the stem cell microenvironment, *Biomaterials*, 2007, **28**, 3208–16.
27 A. Trickett and Y. L. Kwan, T cell stimulation and expansion using anti-CD3/CD28 beads, *J. Immunol. Methods*, 2003, **275**, 251–255.
28 L. Zhou, M. M. W. Chong and D. R. Littman, Plasticity of $CD4^+$ T cell lineage differentiation, *Immunity*, 2009, **30**, 646–55.
29 E. K. Deenick, A. V. Gett and P. D. Hodgkin, Stochastic model of T cell proliferation: a calculus revealing IL-2 regulation of precursor frequencies, cell cycle time, and survival, *Journal of immunology*, 2003, **170**, 4963–72.
30 a. V. Gett and P. D. Hodgkin, A cellular calculus for signal integration by T cells, *Nat. Immunol.*, 2000, **1**, 239–44.
31 E. D. Hawkins, J. F. Markham, L. P. McGuinness and P. D. Hodgkin, A single-cell pedigree analysis of alternative stochastic lymphocyte fates, *Proc. Natl. Acad. Sci. U. S. A.*, 2009, **106**, 13457–62.
32 D. A. Cantrell and K. A. Smith, The interleukin-2 T-cell system: a new cell growth model, *Science*, 1984, **224**, 1312–6.
33 K. M. Smith, J. M. Davidson and P. Garside, T-cell activation occurs simultaneously in local and peripheral lymphoid tissue following oral administration of a range of doses of immunogenic or tolerogenic antigen although tolerized T cells display a defect in cell division, *Immunology*, 2002, **106**, 144–58.
34 Y. Y. Wan and R. A. Flavell, Regulatory T-cell functions are subverted and converted owing to attenuated Foxp3 expression, *Nature*, 2007, **445**, 766–70.
35 M. a. Gavin, *et al.*, Foxp3-dependent programme of regulatory T-cell differentiation, *Nature*, 2007, **445**, 771–5.